

Fig. S1. Enlarged XRD plot of undoped and doped NiO_x thin films showing shift to lower 2θ value with increased dopant concentration

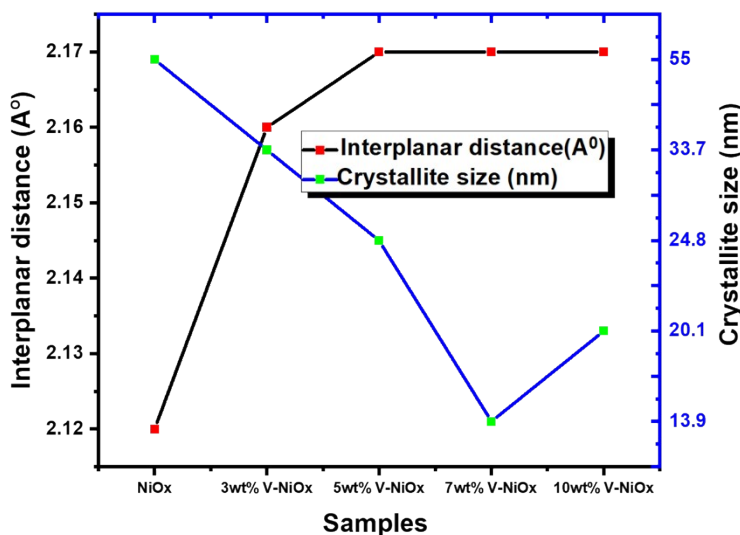


Fig. S2. Comparison plot of interplanar spacing and crystallite size in undoped and different wt. % V doped NiO_x

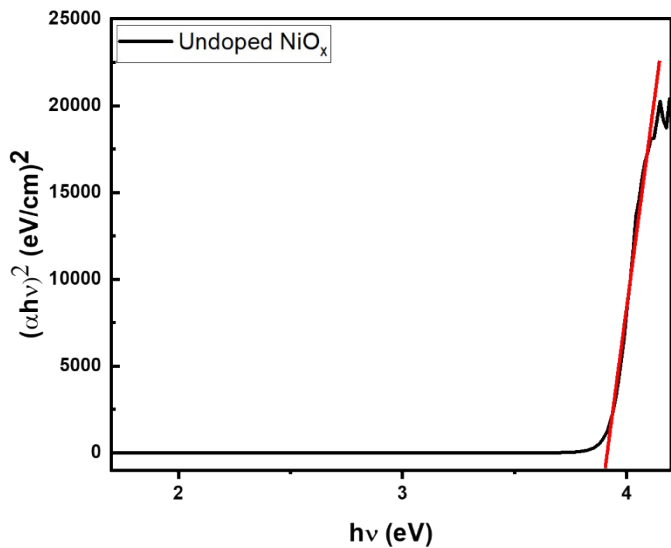


Fig. S3. Tauc plot of undoped NiO_x thin film.

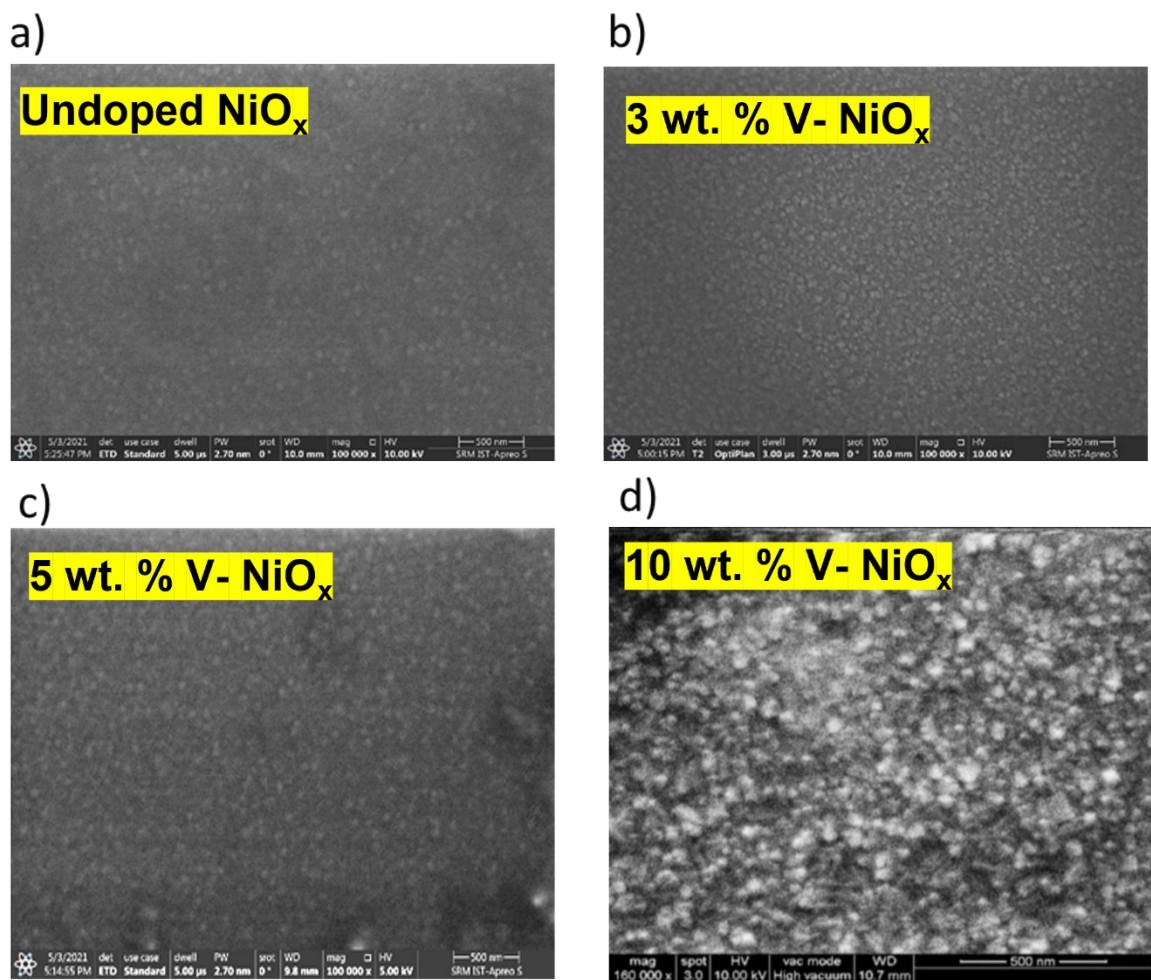


Fig. S4. SEM images of a) undoped NiO_x b) 3wt.% V- NiO_x c) 5wt.% V- NiO_x d) 10wt.% V- NiO_x thin film.

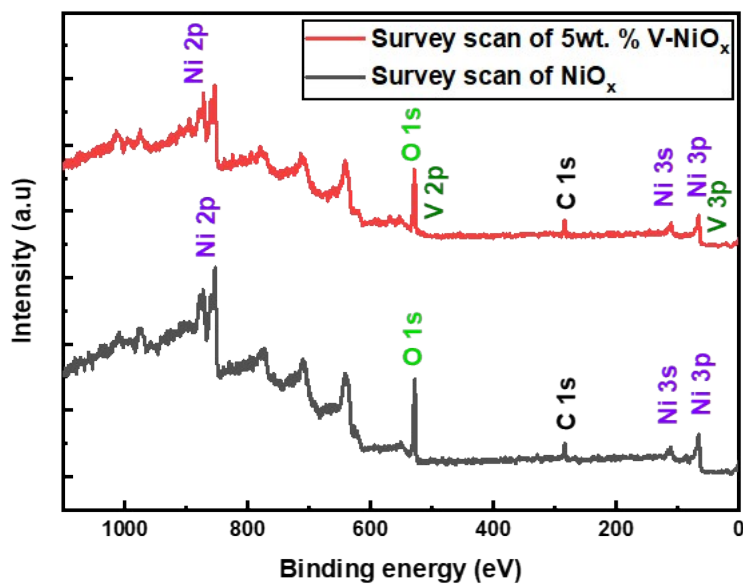


Fig. S5. XPS survey scan for undoped NiO_x and 5 wt. % V doped NiO_x

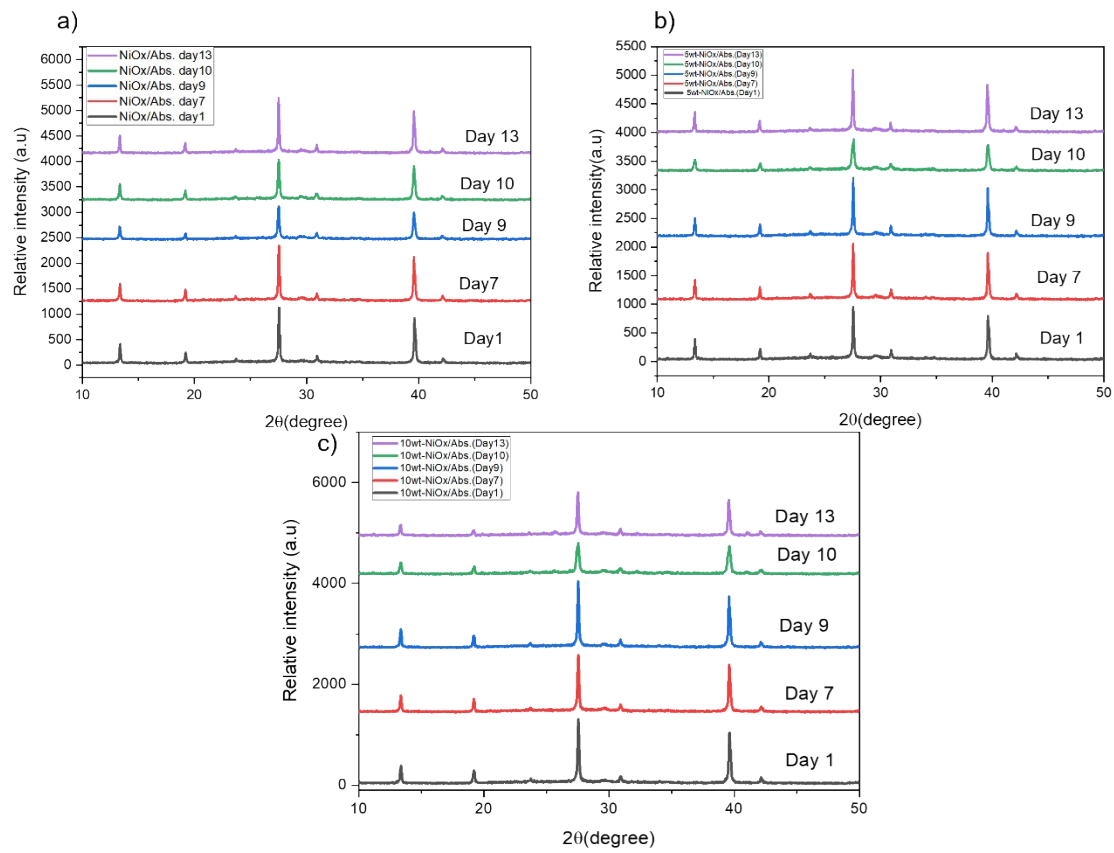


Fig. S6. Degradation analysis of CsFAPbI₃ thin films samples stored in dark, N₂ atmosphere for 13 days. a) CsFAPbI₃ absorber on undoped NiO_x b) CsFAPbI₃ absorber on 5 wt. % V-NiO_x c) CsFAPbI₃ on 10 wt. % V-NiO_x

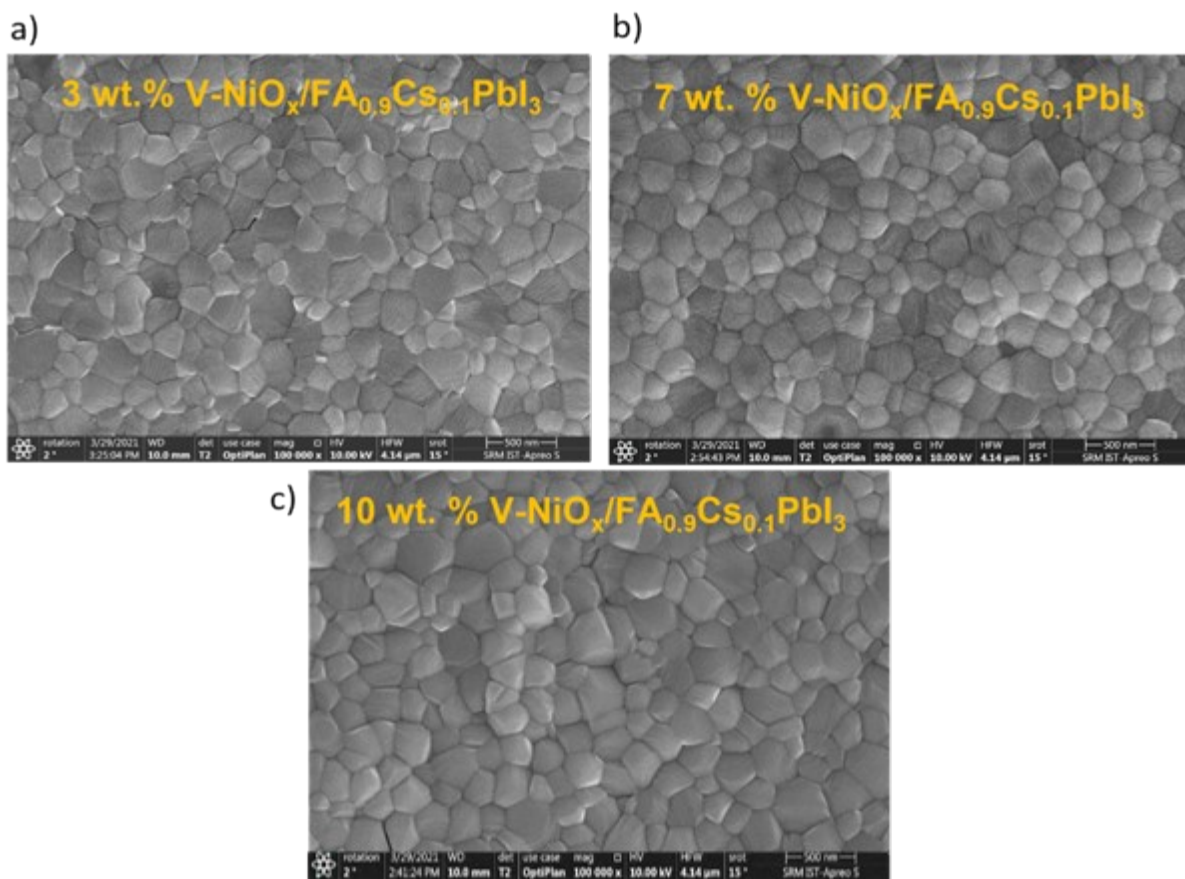


Fig. S7. SEM image of absorber coated on a) 3 wt. % V-NiO_x b) 7 wt. % V-NiO_x and c) 10 wt. % V-NiO_x with inset showing corresponding grain size distribution.

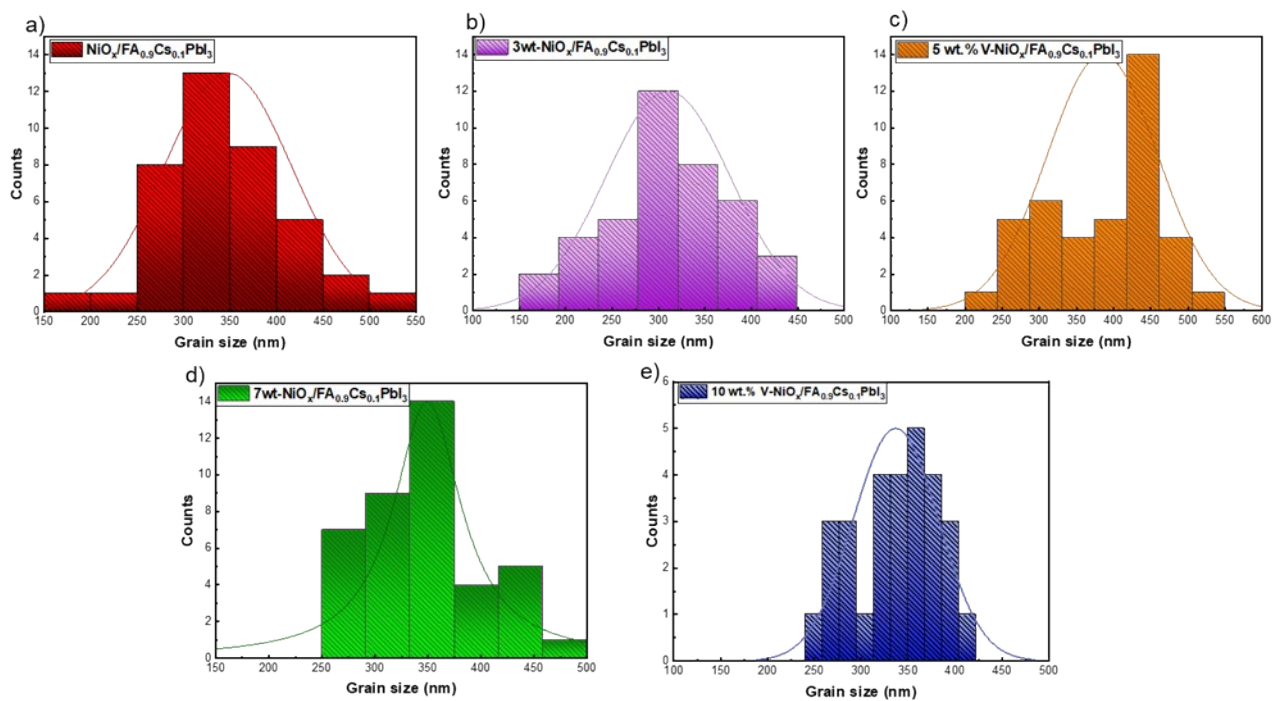


Fig. S8. Grain size histograms of absorber coated on top of a) undoped NiO_x b) 3 wt.% V- NiO_x c) 5 wt.% V- NiO_x d) 7 wt.% V- NiO_x and e) 10 wt.% V- NiO_x .

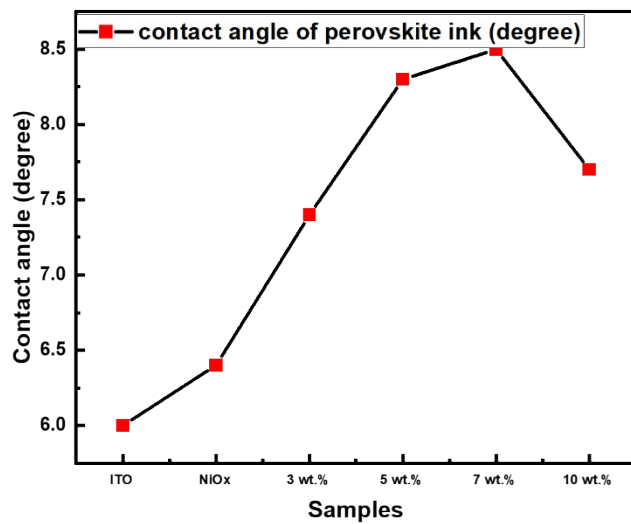


Fig. S9. Contact angle measurement on undoped and different wt. % V doped NiO_x thin films with DMF:DMSO solvent.

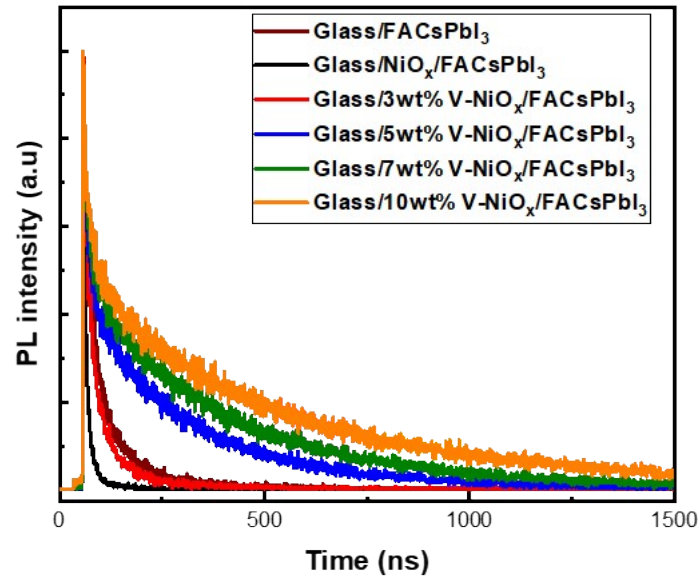


Fig. S10. Time resolved PL spectra of absorber on top of undoped and different wt. % V-doped NiO_x HTL.

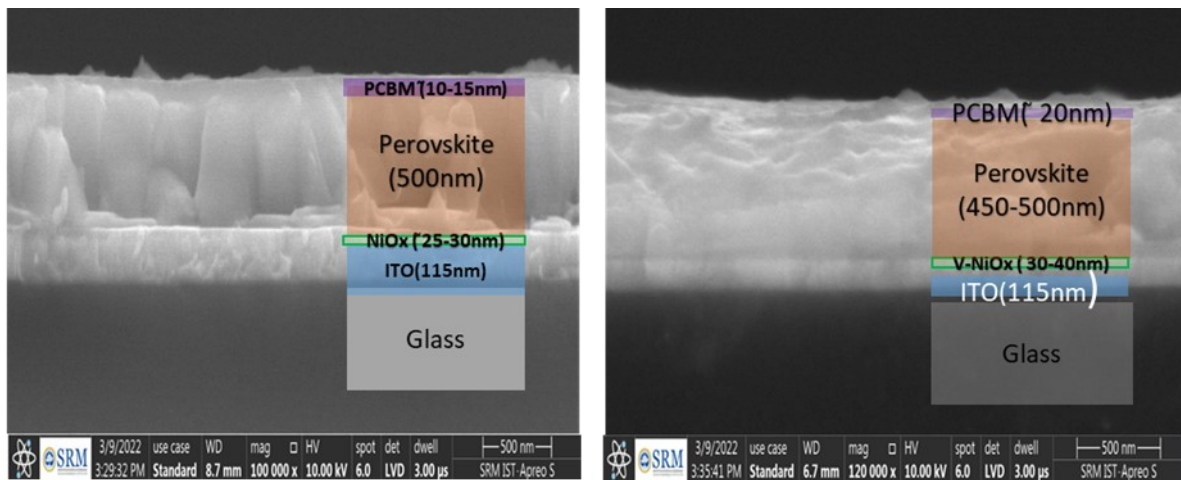


Fig. S11. a) Cross-section SEM images of $\text{FA}_{0.9}\text{Cs}_{0.1}\text{PbI}_3$ absorber on undoped NiO_x HTL b) 5 wt. % V-NiO_x HTL.

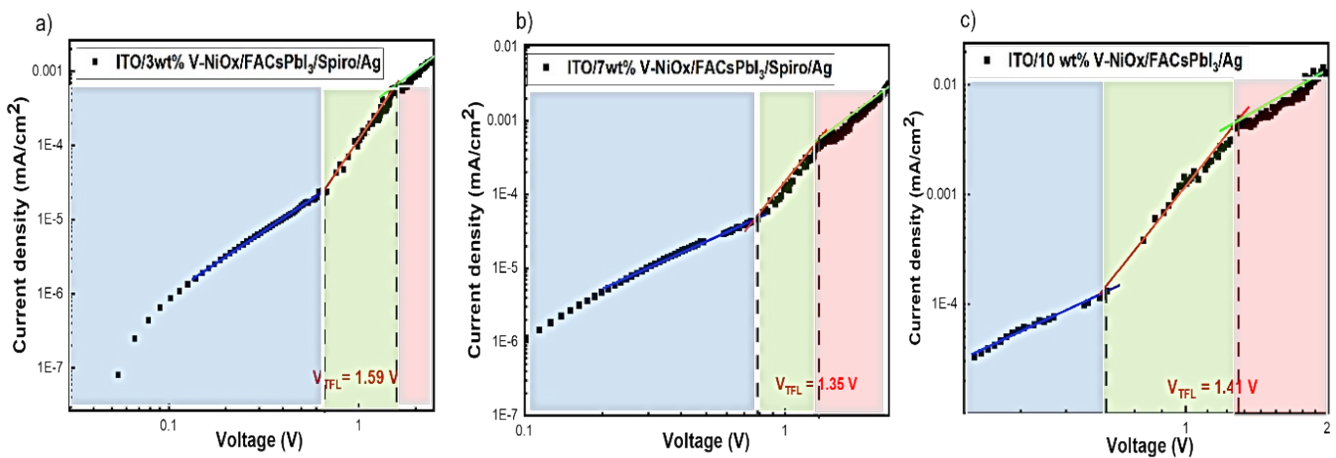


Fig. S12. SCLC plots of a) 3wt. % V-NiO_x b) 7wt. % V-NiO_x and c) 10wt. % V-NiO_x hole only devices.

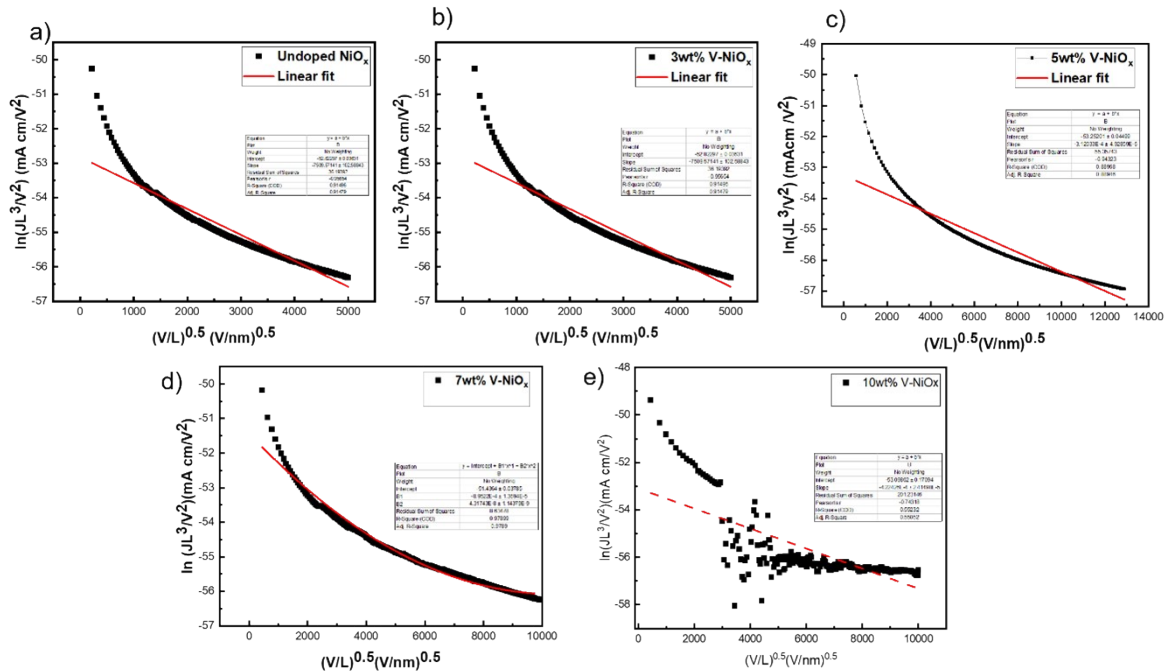


Fig. S13. Mobility plots of a) undoped NiO_x b) 3 wt.% V-NiO_x c) 5 wt.% V-NiO_x d) 7 wt.% V-NiO_x and e) 10 wt.% V-NiO_x.